Evaluation of reduction efficiencies of pepper mild mottle virus and human enteric viruses in full-scale drinking water treatment plants employing coagulation-sedimentation–rapid sand filtration or coagulation–microfiltration

D. Shirakawa, N. Shirasaki*, T. Matsushita, Y. Matsui, R. Yamashita, T. Matsumura, S. Koriki

Division of Environmental Engineering, Faculty of Engineering, Hokkaido University, N13W8, Sapporo 060-8628, Japan

* Corresponding author. Tel.: +81-11-706-7282; fax: +81-11-706-7282.
E-mail address: nobutaka@eng.hokudai.ac.jp (N. Shirasaki)

Abstract

Here, we evaluated the reduction efficiencies of indigenous pepper mild mottle virus (PMMoV, a potential surrogate for human enteric viruses to assess virus removal by coagulation-sedimentation–rapid sand filtration [CS–RSF] and coagulation–microfiltration [C–MF]) and representative human enteric viruses in four full-scale drinking water treatment plants that use CS–RSF (Plants A and B) or C–MF (Plants C and D). First, we developed a virus concentration method by using an electropositive filter and a tangential-flow ultrafiltration membrane to effectively concentrate and recover PMMoV from large volumes of water: the recovery rates of PMMoV were 100% when 100-L samples of PMMoV-spiked dechlorinated tap water were concentrated to 20 mL; even when spiked water volume was 2000 L, recovery rates of >30% were maintained. The concentrations of indigenous PMMoV in raw and treated water samples determined by using this method were always above the quantification limit of the real-time polymerase chain reaction assay. We therefore were able to determine its

reduction ratios: 0.9–2.7-$\log_{10}$ in full-scale CS–RSF and 0.7–2.9-$\log_{10}$ in full-scale C–MF. The PMMoV reduction ratios in C–MF at Plant C (1.0 ± 0.3-$\log_{10}$) were lower than those in CS–RSF at Plants A (1.7 ± 0.5-$\log_{10}$) and B (1.4 ± 0.7-$\log_{10}$), despite the higher ability of MF for particle separation in comparison with RSF owing to the small pore size in MF. Lab-scale virus-spiking C–MF experiments that mimicked full-scale C–MF revealed that a low dosage of coagulant (polyaluminum chloride [PACl]) applied in C–MF, which is determined mainly from the viewpoint of preventing membrane fouling, probably led to the low reduction ratios of PMMoV in C–MF. This implies that high virus reduction ratios (>4-$\log_{10}$) achieved in previous lab-scale virus-spiking C–MF studies are not necessarily achieved in full-scale C–MF. The PMMoV reduction ratios in C–MF at Plant D (2.2 ± 0.6-$\log_{10}$) were higher than those at Plant C, despite similar coagulant dosages. In lab-scale C–MF, the PMMoV reduction ratios increased from 1-$\log_{10}$ (with PACl [basicity 1.5], as at Plant C) to 2–4-$\log_{10}$ (with high-basicity PACl [basicity 2.1], as at Plant D), suggesting that the use of high-basicity PACl probably resulted in higher reduction ratios of PMMoV at Plant D than at Plant C. Finally, we compared the reduction ratios of indigenous PMMoV and representative human enteric viruses in full-scale CS–RSF and C–MF. At Plant D, the concentrations of human norovirus genogroup II (HuNoV GII) in raw water were sometimes above the quantification limit; however, whether its reduction ratios in C–MF were higher than those of PMMoV could not be judged since reduction ratios were ≥1.5-$\log_{10}$ for HuNoV GII and 2.3–2.9-$\log_{10}$ for PMMoV. At Plant B, the concentrations of enteroviruses (EVs) and HuNoV GII in raw water were above the quantification limit on one occasion, and the reduction ratios of EVs (≥1.3-$\log_{10}$) and HuNoV GII (≥1.5-$\log_{10}$) in CS–RSF were higher than that of PMMoV (0.9-$\log_{10}$). This finding supports the usefulness of PMMoV as a potential surrogate for human enteric viruses to assess virus removal by CS–RSF.

Keywords

Coagulation, Microfiltration, Pepper mild mottle virus, Quantitative real-time PCR, Rapid sand filtration, Virus concentration method.

1. Introduction

Human enteric viruses are pathogens that mainly cause gastrointestinal illnesses, and their infective doses are typically low (1–100 particles; WHO, 2011). Because surface waters are frequently contaminated with these viruses (Health Canada, 2017; WHO, 2011), use of such contaminated waters as sources of drinking water production may lead to the spread of waterborne viral diseases if drinking water treatment processes are inadequate for virus reduction (i.e., removal, inactivation, or both). Accordingly, evaluating virus reduction efficiency in drinking water treatment processes and conducting adequate treatment for effective virus reduction are needed to prevent waterborne viral diseases and supply safe drinking water.

Lab-scale experiments using virus-spiked water have been widely used to investigate virus reduction efficiency in drinking water treatment processes (Abbaszadegan et al., 2007; Fiksdal and Leiknes, 2006; Kato et al., 2018; Matsui et al., 2003; Matsushita et al., 2013; Shirasaki et al., 2017a, 2018; Zhu et al., 2005). However, it is unclear whether virus reduction ratios (ratios of virus concentrations before and after treatment) obtained in lab-scale experiments are actually achieved in full-scale drinking water treatment plants (DWTPs). Thus, full-scale studies are needed to investigate virus reduction efficiency in drinking water treatment processes.

Evaluation of virus reduction efficiency in full-scale DWTPs requires quantification of the concentrations of indigenous viruses in raw and treated water. The concentrations of indigenous human enteric viruses in water samples, especially in treated water samples, are usually below the quantification limit of the real-time polymerase chain reaction (PCR) assay, and concentrating these viruses from water is necessary before virus quantification. The concentrations of indigenous human

enteric viruses in raw water can be quantified by applying an appropriate virus concentration method, whereas those in treated water are still nearly always below the quantification limit even when >1000 L of water are concentrated to several milliliters (Sylvestre et al., 2021; Varughese et al., 2018); in many cases, this makes it impossible to evaluate virus reduction efficiency in full-scale DWTPs.

In surface waters, including drinking water sources, the concentrations of the plant virus, pepper mild mottle virus (PMMoV), are higher than those of human enteric viruses (Hamza et al., 2011; Haramoto et al., 2013). Thus, the concentrations of indigenous PMMoV not only in raw but also in treated water can be quantified, which makes it possible to evaluate its reduction efficiencies in full-scale DWTPs. In addition, our research group has reported that the reduction ratios of PMMoV are similar to or lower than those of human enteric viruses in lab-scale virus-spiking coagulation-sedimentation–rapid sand filtration (CS–RSF) and low-pressure membrane (LPM) filtration experiments (Shirasaki et al., 2017a, 2018). Accordingly, when the reduction ratios of indigenous PMMoV in full-scale CS–RSF and LPM filtration are successfully determined by applying an appropriate virus concentration method, similar or higher reduction ratios could be expected for human enteric viruses.

CS–RSF is used worldwide in full-scale DWTPs, mainly to reduce turbidity. Virus reduction efficiency in full-scale CS–RSF has been successfully determined by targeting indigenous PMMoV, and reduction ratios of 1.7–2.9-$\log_{10}$, as evaluated by PCR assay, have been reported (Asami et al., 2016; Kato et al., 2018). Application of LPM technology including microfiltration (MF) to drinking water treatment has increased dramatically (Huang et al., 2009). A combination of coagulation pretreatment and MF (coagulation–MF [C–MF]) has been widely used at full-scale DWTPs because coagulation is the most successful pretreatment for MF to mitigate membrane fouling (Huang et al., 2009). In previous lab-scale virus-spiking C–MF studies, including those of our research group, virus reduction ratios of >4-$\log_{10}$ are achieved under appropriate coagulation conditions (Fiksdal and Leiknes, 2006; Matsui et al., 2003; Matsushita et al., 2013; Shirasaki et al., 2017a; Zhu et al., 2005).

However, virus reduction efficiency in full-scale C–MF has not yet been investigated. Thus, it is unclear whether the high virus reduction ratios obtained in lab-scale C–MF are actually achieved in full-scale C–MF.

Although numerous virus concentration methods have been developed and used to quantify virus concentrations in water, a standard method that can effectively concentrate all viruses from various types of water has not yet been established (Haramoto et al., 2018). Currently, membrane-based virus concentration methods are commonly applied to concentrating viruses from water (Shi et al., 2017). An electronegative filter-based method is widely used to concentrate indigenous viruses from water (Haramoto et al., 2018). In fact, this method has been applied to concentrating indigenous PMMoV in raw and treated water in full-scale CS–RSF (Asami et al., 2016; Kato et al., 2018). However, virus recovery efficiencies and the extent of inhibition of the PCR assay depend on virus concentration method, virus type, sample volume, and water quality (Haramoto et al., 2018). Accordingly, application of a virus concentration method other than the electronegative filter-based method is needed to accumulate data on virus reduction efficiency in full-scale CS–RSF, which contributes to determining how much log credit for virus reduction is allocable to CS–RSF.

An electropositive filter-based method is also widely used to concentrate indigenous viruses from water (Haramoto et al., 2018); unlike the electronegative filter-based method, it does not require the addition of multivalent cations prior to concentration, making it easy to concentrate viruses on-site from large volumes of water. The U.S. Environmental Protection Agency has proposed an electropositive filter-based method to concentrate two types of human enteric viruses, enteroviruses (EVs) and noroviruses (Method 1615; Fout et al., 2014). Method 1615 effectively concentrates poliovirus (PV; included in EVs) and murine norovirus (MNV), a surrogate of human noroviruses, from large volumes of water: the recovery rates of these viruses, as evaluated by the PCR assay, were ≥20% when 1500–1900 L of groundwater followed by 10 L of PV- and MNV-spiked groundwater were filtered and concentrated to 400 μL (Cashdollar et al., 2013). However, human enteric viruses

126 are round-shaped (20–70 nm in diameter), whereas PMMoV is rod-shaped (18 nm × 300–310 nm;
127 Fauquet et al., 2005). Thus, it remains unclear whether Method 1615 can effectively concentrate
128 PMMoV along with human enteric viruses from water. In fact, Shi et al. (2017) have suggested that
129 physicochemical properties of viruses (e.g., size, shape, and surface charge) can affect virus recovery
130 efficiencies.

131 In the present study, we first tested a slightly modified version of Method 1615 to concentrate
132 PMMoV from large volume of water, but the recovery rate was very low (0.7%) when 1000 L of
133 PMMoV-spiked dechlorinated tap water was concentrated to 20 mL. To effectively concentrate and
134 recover PMMoV along with human enteric viruses from large volumes of water compared with
135 Method 1615, we developed a virus concentration method by using an electropositive filter and a
136 tangential-flow ultrafiltration (TF-UF) membrane. We then used the developed virus concentration
137 method to evaluate the reduction efficiencies of indigenous PMMoV and representative human
138 enteric viruses (adenovirus [AdV], EVs, hepatitis A virus [HAV], and human norovirus genogroups I
139 and II [HuNoVs GI and GII]) in four full-scale DWTPs, two employing CS–RSF and two employing
140 C–MF. In addition, we conducted lab-scale virus-spiking CS–RSF and C–MF experiments that
141 mimicked full-scale CS–RSF and C–MF to validate the virus reduction ratios observed in full-scale
142 CS–RSF and C–MF.

143

144 **2. Materials and methods**

145

146 *2.1. Plant viruses, human enteric viruses, MNV, and a bacteriophage*

147

148 Two plant viruses, PMMoV pepIwateHachiman1 strain (MAFF 104099) and cucumber green
149 mottle virus (CGMMV) SH strain (MAFF 260018), were obtained from the National Institute of
150 Agrobiological Sciences Genebank (Tsukuba, Japan). AdV type 40 Dugan strain (ATCC VR-931),

coxsackievirus (CV) B5 Faulkner strain (ATCC VR-185), HAV IB HM175/18f strain (ATCC VR-1402), and MNV type 1 CW1 strain (ATCC PTA-5935) were obtained from the American Type Culture Collection (ATCC, Manassas, VA, USA). F-specific RNA bacteriophage MS2 (NBRC 102619) was obtained from the National Institute of Technology and Evaluation Biological Resource Center (Kisarazu, Japan). Details of propagation and purification of PMMoV, AdV, CV, HAV, MNV, and MS2 are described in our previous reports (Shirasaki et al., 2016, 2017b, 2018). CGMMV was propagated in the same way as PMMoV.

AdV, CV, and HAV were used as representative human enteric viruses, and MNV was used as a surrogate for human caliciviruses for the assessment of the efficacy of the virus concentration method to concentrate and recover human enteric viruses. In addition, CGMMV, MNV, and MS2 were used as process control viruses, because CGMMV is phylogenetically and morphologically similar to PMMoV (both belong to the genus *Tobamovirus* in the family Virgaviridae; Fauquet et al., 2005), and because MNV and MS2 are widely used as process control viruses (Haramoto et al., 2018; Shi et al., 2017).

2.2. Virus quantification by real-time PCR or real-time reverse-transcription PCR

Viral DNA of AdV was quantified by real-time PCR, and viral RNA of PMMoV, CGMMV, EVs including CV, HAV, HuNoVs GI and GII, MNV, or MS2 was quantified by real-time reverse-transcription PCR (real-time RT-PCR), as described in the Supplementary Information (Section S1.1, Table S1).

2.3. Virus concentration method

Each water sample (4–2000 L) was filtered through an electropositive filter (NanoCeram cartridge filter P2.5-5DP or VS2.5-5; Argonide, Sanford, FL, USA) at an initial flow rate of 2–6 L/min by using a magnetic pump. The virus was eluted from the filter with 1.5% (w/w) beef extract (Becton, Dickinson and Company, Franklin Lakes, NJ, USA) solution containing 0.05 M glycine (hereafter "BE solution", pH 9.0 or 9.5) as follows. Approximately 350 mL of BE solution was added onto the filter in a designated housing to cover the filter completely, the filter was allowed to soak, and then the BE solution was passed through the filter together with newly added 150 mL of BE solution at approximately 1.5 L/min by a peristaltic pump. The eluate (500 mL) was collected into a sterilized glass beaker. Elution was performed four times: the soaking times before the four elution steps were (1) 1 min, (2) 15 min, (3) 15 or 30 min, and (4) 15 or 30 min. All eluates (2 L in total) were collected in the same beaker. The pH was adjusted to 3.5 with HCl, and the eluate was mixed with a sterilized magnetic stirrer at 400 rpm for 30 min to generate BE floc particles (organic flocculation). The floc mixture was centrifuged at 2500 × *g* for 15 min to separate the flocs from the mixture. The supernatant (2 L) was collected in the beaker, and its pH was adjusted to 7.0 with NaOH. The supernatant was then concentrated to 20 mL by means of a TF-UF cassette (Pellicon XL; nominal molecular weight cutoff, 300 kDa; regenerated cellulose; Millipore Corp., Billerica, MA, USA), and filtered through a hydrophilic cellulose acetate membrane filter (nominal pore size, 0.45 μm; Dismic-25CS, Toyo Roshi Kaisha, Tokyo, Japan). The resultant sample is referred to as the "supernatant concentrated sample". The floc pellet was dissolved in 20 mL of 0.15 M sodium phosphate buffer (pH 9.0), centrifuged at 4000 × *g* for 10 min to collect the dissolved solution completely; the dissolved solution (20 mL) was collected into another sterilized glass beaker, its pH was adjusted to 7.0 with HCl, and it was filtered through the hydrophilic cellulose acetate membrane filter. The resultant sample is referred to as the "floc dissolution sample". Virus concentrations in both samples were quantified, and their sum was considered as virus concentration in each concentrated sample.

200 *2.4. Full-scale studies*

201

202 *2.4.1. Sample collection and concentration in full-scale DWTPs*

203

204 All four DWTPs are located in Japan. Plants A and B employ CS–RSF, and Plants C and D employ
205 C–MF. Water samples were collected and concentrated at Plant A from October 2017 to February
206 2019, Plant B from November 2017 to February 2019, Plant C from May 2018 to July 2019, and
207 Plant D from July 2020 to March 2021. Detailed information about the four DWTPs and samples is
208 provided in Section S1.2 and Table S2.

209 Water samples (4–2000 L) were concentrated on-site by filtering through the NanoCeram filter at
210 an initial flow rate of 2–6 L/min by using the magnetic pump. To dechlorinate water after chlorination
211 (samples after RSF at Plant A; after CS and primary RSF at Plant B in February 2019; after pre-
212 chlorination, manganese oxide [MnOx]-coated media filtration, and C–MF at Plant C; and after
213 coagulation and MF at Plant D), sodium thiosulfate was injected in-line by the peristaltic pump before
214 filtration of water through the NanoCeram filter to a final concentration of 50 mg/L. After on-site
215 filtration, the NanoCeram filters were transferred to our laboratory at Hokkaido University at 4 °C,
216 and stored at 4 °C. Virus elution from the filter was conducted immediately after the filter was brought
217 to 20 °C.

218 Water samples for virus-spiking experiments (see Sections 2.4.3 and 2.5) were collected in plastic
219 containers on on-site sampling days. The samples were stored at 4 °C until use, and brought to 20 °C
220 immediately prior to use.

221

222 *2.4.2. Calculation of virus reduction ratio in full-scale DWTPs*

223

The concentrations of indigenous PMMoV and representative human enteric viruses (AdV, EVs, HAV, and HuNoVs GI and GII), included in the Drinking Water Contaminant Candidate List 4 (USEPA, 2016), were quantified in the on-site concentrated samples. Undiluted samples or samples diluted 10-fold with sterilized DNase/RNase-free distilled water were used for virus quantification. The virus reduction ratios were calculated by dividing the virus concentrations before (C_0) by those after (C) treatment. Comparison of the virus reduction ratios between DWTPs was performed using Student's *t*-test, with *P*-values less than 0.05 being considered statistically significant.

2.4.3. Assessment of the usefulness of the developed virus concentration method for raw and treated water in full-scale DWTPs

The usefulness of the developed virus concentration method for raw and treated water in full-scale DWTPs was assessed as follows. (1) The raw and treated water samples collected at full-scale DWTPs were spiked with the known amounts of viruses, concentrated, and the total recovery rates of the viruses from the spiked samples were evaluated. (2) The on-site concentrated samples were spiked with the known amounts of viruses, and the quantification efficiencies (i.e., the RNA extraction, RT, and real-time PCR efficiencies) of the viruses in the spiked samples were evaluated (for details, see Sections S1.3 and S1.4).

2.5. Lab-scale virus-spiking CS–RSF and C–MF experiments

To validate the virus reduction ratios observed in full-scale CS–RSF and C–MF, we conducted lab-scale virus-spiking CS–RSF and C–MF experiments with the water samples collected at Plants A, B, and C. To mimic full-scale CS–RSF (Plants A and B) and C–MF (Plant C), we used the same sulfated polyaluminum chloride (PACl) products with basicity ($[OH^-]/[Al^{3+}]$) 1.5 (PACl-1.5s) as used at the

three DWTPs as coagulants; they are specified in Section S1.5. To mimic full-scale CS–RSF, we used silica sand or manganese sand (effective size, 0.6 mm; uniformity coefficient, <1.3; Nihon Genryo Co., Kawasaki, Japan) as the filter medium for RSF. To mimic full-scale C–MF, where a hollow-fiber membrane module (nominal pore size, 0.1 μm; polyvinylidene difluoride) is installed, we used a commercially available lab-scale MF membrane module (effective filtration area, 0.012 m^2; Microza, Asahi Kasei, Tokyo, Japan) that consists of the same hollow-fiber membrane as used at Plant C. Details of experimental procedures are described in Sections S1.6 and S1.7.

3. Results and discussion

3.1. Development of a virus concentration method

First, we filtered and concentrated 1000 L of PMMoV-spiked dechlorinated tap water by using Method 1615 with slight modifications (different filter type and four elutions instead of two; see Section S1.8 for details of experimental procedures; see legend to Table 1 for the description of Method 1615). The total recovery rate (R_t) of PMMoV (0.7%; Table 1, Method 1) was far below acceptable total virus recovery rates in Method 1615 (5%−200%; Fout et al., 2014). A retention rate (R_r) of 95% and elution rate (R_e) of 28% for PMMoV did not fully explain its low total recovery rate; therefore, organic flocculation was the most-likely cause. Accordingly, we conducted virus-spiking organic flocculation experiments to investigate the efficacy of organic flocculation in concentrating and recovering viruses from eluates (for details of experimental procedures, see Section S1.9). We found that CGMMV, human enteric viruses (AdV, CV, and HAV), and MNV were recovered mainly in floc dissolution samples, whereas PMMoV and MS2 mostly remained in the supernatant of the floc mixture (Fig. 1). This result indicated that the low total recovery rate of PMMoV was due to its poor recovery during organic flocculation. Proteins in the BE solution self-flocculate at pH around

3.5, and viruses are entrapped in BE flocs during organic flocculation (Katzenelson et al., 1976). The isoelectric points of PMMoV (3.2) and MS2 (2.2; Shirasaki et al., 2016, 2017a) are <3.5, whereas that of CGMMV (4.3; Sano et al., 1978) and those of AdV, CV, HAV, and MNV (3.6–3.8; Shirasaki et al., 2016, 2017b) are >3.5. Thus, viral surface charges at pH 3.5 were probably different between viruses with isoelectric points of <3.5 and >3.5, and the difference in viral surface charges at pH 3.5 possibly determined whether the viruses were recovered in floc dissolution samples or remained in the supernatant.

To effectively concentrate and recover PMMoV, we further concentrated the supernatant of the floc mixture using a TF-UF membrane with a nominal molecular weight cutoff of 300 kDa, which is much smaller than the molecular weight of PMMoV (40×10^3 kDa; Fauquet et al., 2005). The total recovery rates of PMMoV were markedly increased from 0.7% to 49%–80% by adding the TF-UF process to the virus concentration processes (Table 1, Methods 2–4). In addition, the elution rate of PMMoV increased as the pH of BE solution was increased from 9.0 to 9.5 (Table 1, Method 3), indicating that the pH of BE solution affected the elution rate of PMMoV. In contrast, filter type, and soaking times for the third and fourth elution did not affect the retention and elution rates of PMMoV, and consequently did not affect its total recovery rate (Table 1, Methods 2 and 4). Details of the effects of filter type and elution conditions on virus recovery rates are described in Section S2.1. On the basis of these findings, we concluded that Method 4 was optimal for concentrating PMMoV in our trials, and used it in subsequent experiments.

To investigate the effect of filtration volume on virus recovery rates, we filtered and concentrated 100–2000 L of PMMoV-spiked dechlorinated tap water (Fig. 2). Regardless of filtration volume, the retention rates of PMMoV were very high (94%–100%), indicating that the NanoCeram filter retained almost all PMMoV even at the maximum volume tested. The total recovery rate of PMMoV was 108% when 100 L of spiked water was concentrated, indicating that the developed virus concentration method completely recovered PMMoV from 100 L of the spiked water. With increasing filtration

volume to 500–2000 L, total recovery rates were decreased, but maintained at 33%–42%. Whereas the elution rates of PMMoV (≥87%) and its recovery rates in the supernatant of the floc mixture (≥73%) were almost independent of filtration volume, the recovery rates of PMMoV by TF-UF were decreased from 150% to 39%–56% with increasing filtration volume from 100 to 500–2000 L (data not shown). This result indicates that the decrease in the total recovery rate of PMMoV was due to the decrease in its recovery rate by TF-UF. We also confirmed that the developed method can effectively concentrate and recover PMMoV along with MNV, which is recovered mainly in floc dissolution samples as described above, from large volumes of dechlorinated tap water (discussed in detail in Section S2.2). These results suggest that the developed method combining organic flocculation and TF-UF can effectively concentrate not only viruses that are recovered mainly in floc dissolution samples (e.g., human enteric viruses) but also viruses that mostly remain in the supernatant of floc mixture (e.g., PMMoV) from large volumes of water.

3.2. Usefulness of the developed virus concentration method for raw and treated water in full-scale DWTPs

As described above, the developed virus concentration method can effectively concentrate and recover PMMoV along with MNV from large volumes of dechlorinated tap water. In general, water quality can affect virus recovery efficiencies during virus concentration processes (Haramoto et al., 2018). In addition, inhibitory substances against the PCR assay that were originally present in water samples could be co-concentrated with viruses, and interfere with virus quantification. To assess the usefulness of the developed method for raw and treated water in full-scale DWTPs, we evaluated the total recovery rates of viruses from spiked raw and treated water samples collected at full-scale DWTPs, and the quantification efficiencies of viruses in spiked on-site concentrated samples. The total recovery rates were ≥79% for PMMoV and ≥17% for the process control viruses (CGMMV,

MNV, and MS2) in all samples tested (Fig. S1). This result suggests that the developed method can effectively concentrate and recover not only viruses that are recovered mainly in floc dissolution samples but also viruses that mostly remain in supernatant concentrated samples derived from raw and treated water in full-scale DWTPs.

Quantification efficiencies (E_q) of the process control viruses (CGMMV, MNV, and MS2) in on-site concentrated samples are shown in Fig. S2. Supernatant concentrated samples, in which PMMoV mostly remained, showed quantification efficiencies of ≥30% for the process control viruses even when the samples were tested without dilution, indicating that inhibition of the PCR assay was negligible when PMMoV was concentrated by using the developed virus concentration method. Accordingly, we adopted the concentrations of indigenous PMMoV quantified without dilution of the concentrated samples. The difference between the concentrations of indigenous PMMoV quantified with 10-fold dilution and without dilution was <0.5-$\log_{10}$ (Fig. S3). On the other hand, floc dissolution samples, in which human enteric viruses were recovered mainly, occasionally showed quantification efficiencies of <10% when samples were tested without dilution. Quantification efficiencies for those samples increased to ≥42% when 10-fold dilution was used. Accordingly, if the concentrations of indigenous human enteric viruses quantified with 10-fold dilution were >0.5-$\log_{10}$ higher than those quantified without dilution, we judged that the PCR assay was considerably inhibited, and adopted the concentrations quantified with 10-fold dilution as the concentrations in the concentrated samples; otherwise, we adopted those quantified without dilution. At 100-fold dilution, quantification efficiencies increased to 72%–115% for supernatant concentrated samples and to 82%–132% for floc dissolution samples. This result indicates that inhibition of the PCR assay can be completely mitigated by 100-fold dilution. Thus, 100-fold dilution before virus quantification in virus concentration experiments (described in Sections 3.1 and 3.2) was reasonable to completely mitigate inhibition of the PCR assay.

3.3. Reduction of indigenous PMMoV in full-scale DWTPs employing CS–RSF and C–MF

Next, we evaluated the reduction efficiencies of indigenous viruses in full-scale DWTPs by applying the developed virus concentration method. Indigenous PMMoV was always quantified not only in raw but also in treated water (i.e., its concentrations were above the quantification limit of the PCR assay in all of the raw and treated water samples tested; Fig. 3). We therefore successfully determined the reduction ratios ($\log_{10}[C_0/C]$) of indigenous PMMoV in full-scale DWTPs. At Plants A and B, the concentrations of indigenous PMMoV were decreased by CS and RSF (Fig. 3a and 3b). The reduction ratios of PMMoV were 0.6–1.5-$\log_{10}$ in CS and −0.1–1.4-$\log_{10}$ in RSF at Plant A, and 0.4–1.0-$\log_{10}$ in CS and 0.5–1.2-$\log_{10}$ in RSF at Plant B; reduction ratios of 1.3–2.7-$\log_{10}$ at Plant A and 0.9–2.2-$\log_{10}$ at Plant B were observed in CS–RSF. The reduction ratios of PMMoV in full-scale CS–RSF determined by using the developed method (i.e., the electropositive filter-based method) roughly corresponded to the previously-reported reduction ratios of PMMoV in full-scale CS–RSF determined by using the electronegative filter-based method (1.7–2.9-$\log_{10}$; Asami et al., 2016; Kato et al., 2018). Thus, virus reduction ratios of 1–3-$\log_{10}$ could be expected in full-scale CS–RSF.

At Plant C, the concentrations of indigenous PMMoV in treated water after pre-chlorination and MnOx-coated media filtration (including intermediate-chlorination) were almost the same as those in raw water (Fig. 3c), suggesting that the contributions of these processes to reduction of PMMoV was negligible. Our research group has recently reported that PMMoV has very high resistance to chlorine treatment, probably due to its robust capsid structure: almost no reduction of the PCR signal (i.e., almost no degradation of the viral genetic material) was observed within CT values (chlorine concentration multiplied by contact time) of approximately <80 mg-Cl_2·min/L (Shirasaki et al., 2020). This high resistance probably resulted in almost no reduction of PMMoV by pre- and intermediate-chlorination, because CT values of pre- and intermediate-chlorination are <20 and <30 mg-Cl_2·min/L,

373 respectively. In contrast, the concentrations of indigenous PMMoV were decreased by C–MF, and the
374 PMMoV reduction ratios of 0.7–1.5-$\log_{10}$ were observed in C–MF.

375 At Plant D, the concentrations of indigenous PMMoV in treated water after pre-chlorination,
376 powdered activated carbon adsorption, and coagulation were almost the same as those in raw water
377 (Fig. 3d), suggesting that the contributions of pre-chlorination and powdered activated carbon
378 adsorption to reduction of PMMoV were negligible. This is consistent with the fact that a CT value
379 of pre-chlorination is <70 mg-Cl_2·min/L, and supported by quantification of PMMoV concentrations
380 in the liquid phase of coagulated water samples before and after removing powdered activated carbon
381 (details are described in Section S2.3; Fig. S4). In contrast, the concentrations of indigenous PMMoV
382 were decreased by C–MF, and the PMMoV reduction ratios of 1.3–2.9-$\log_{10}$ were observed in C–MF.

383 We expected higher virus reduction ratios in C–MF than in CS–RSF, because the ability of MF for
384 particle separation is higher than that of RSF owing to the small pore size in MF. However, the
385 reduction ratios of PMMoV in C–MF at Plant C (1.0 ± 0.3-$\log_{10}$) were significantly lower ($P < 0.05$)
386 than those in CS–RSF at Plant A (1.7 ± 0.5-$\log_{10}$), and tended to be lower than those in CS–RSF at
387 Plant B (1.4 ± 0.7-$\log_{10}$). In general, coagulation conditions differ greatly between CS–RSF and C–
388 MF: the conditions used in CS–RSF are determined mainly from the viewpoint of turbidity reduction,
389 whereas the conditions used in C–MF are determined mainly from the viewpoint of preventing
390 membrane fouling because MF can completely remove turbidity without coagulation pretreatment
391 due to its high ability for particle separation. On the other hand, coagulation conditions have been
392 shown to affect virus reduction efficiency in previous lab-scale virus-spiking C–MF studies: due to
393 small diameters of viruses compared with nominal pore sizes of MF membranes, only limited virus
394 reduction ratios (<1-$\log_{10}$) were obtained without coagulation pretreatment or under inappropriate
395 coagulation conditions, whereas virus reduction ratios of >4-$\log_{10}$ were obtained under appropriate
396 coagulation conditions (Fiksdal and Leiknes, 2006; Matsui et al., 2003; Matsushita et al., 2013;
397 Shirasaki et al., 2017a; Zhu et al., 2005). Thus, the lower reduction ratios of PMMoV in C–MF at

Plant C than in CS–RSF at Plants A and B could be attributed to the difference in coagulation conditions. The reduction ratios of PMMoV in C–MF at Plant D (2.2 ± 0.6-$\log_{10}$) were significantly higher ($P < 0.05$) than those at Plant C. Because the nominal pore sizes of membranes installed at Plants C and D are the same (0.1 μm; see Section S1.3), the difference in coagulation conditions between these DWTPs could contribute to this difference. The reasons for the lower reduction ratios of PMMoV in C–MF at Plant C than in CS–RSF at Plants A and B, and the reasons for the higher reduction ratios of PMMoV in C–MF at Plant D than at Plant C are further discussed in Section 3.4.

3.4. Lab-scale virus-spiking CS–RSF and C–MF experiments to mimic full-scale CS–RSF and C–MF

To validate the virus reduction ratios observed in full-scale CS–RSF and C–MF, we conducted lab-scale virus-spiking CS–RSF and C–MF experiments. The reduction ratios of PMMoV at lab-scale experiments were similar to those in full-scale studies at similar coagulant dosages, except in raw water sample collected at Plant A in July 2018 (Fig. 4). This result indicated that virus reduction in lab-scale CS–RSF and C–MF successfully mimicked that in full-scale CS–RSF and C–MF, except in the above case (discussed in detail in Sections S2.4 and S2.5; Fig. S5). Accordingly, we investigated the effects of coagulation conditions on virus reduction in lab-scale CS–RSF and C–MF to elucidate why PMMoV reduction ratios were lower in C–MF at Plant C than in CS–RSF at Plants A and B, and why PMMoV reduction ratios were higher in C–MF at Plant D than at Plant C.

In lab-scale CS–RSF with raw water sample collected at Plant A in February 2019, the reduction ratio ($[\log_{10}[C_{c0}/C_{cs}] + \log_{10}[C_{r0}/C_{rf}]$) of PMMoV was 3.6-$\log_{10}$ at a coagulant dosage of 1.62 mg-Al/L (similar to 1.51 mg-Al/L used at Plant A; Fig. 4a), but decreased to 0.5-$\log_{10}$ at 0.54 mg-Al/L. In raw water sample from Plant B, the reduction ratio was 2.9-$\log_{10}$ at 1.08 mg-Al/L (similar to 0.98 mg-Al/L used at Plant B; Fig. 4b), but decreased to 1.8-$\log_{10}$ at 0.54 mg-Al/L. In lab-scale C–MF with water samples from Plant C, the reduction ratios ($\log_{10}[C_{m0}/C_{mf}]$) of PMMoV were only 0.5–

1.1-$\log_{10}$ at 0.27 mg-Al/L (similar to 0.33 or 0.27 mg-Al/L used at Plant C; Fig. 4c), but markedly increased to 2.8–3.5-$\log_{10}$ at 0.54 mg-Al/L. These results indicate that coagulant dosage affected virus reduction efficiency in CS–RSF and C–MF, and that low coagulant dosage used in C–MF at Plant C (0.3–0.4 mg-Al/L on the sampling days) was a reason for the lower PMMoV reduction ratios in C–MF at Plant C than in CS–RSF at Plants A and B.

At lab-scale experiments at 0.54 mg-Al/L, the reduction ratios of PMMoV in C–MF (2.8–3.5-$\log_{10}$) were higher than those in CS–RSF (0.5–1.8-$\log_{10}$), indicating that C–MF has higher ability for virus reduction than CS–RSF. On the other hand, coagulant dosages used in C–MF are typically lower than those used in CS–RSF; because MF has high ability for particle separation, the aim of coagulation pretreatment in MF is mainly to prevent membrane fouling, not to reduce turbidity like in RSF. This implies that high virus reduction ratios compared with those achieved in full-scale CS–RSF are not necessarily achieved in full-scale C–MF, despite its higher ability for virus reduction in comparison with CS–RSF. Therefore, control of coagulation conditions, including coagulant dosage, is of great importance for actually achieving high virus reduction ratios in full-scale C–MF.

As described in Section 3.3, the reduction ratios of PMMoV in C–MF were higher at Plant D than at Plant C, despite similar coagulant dosages (0.3–0.6 mg-Al/L on the sampling days) at both DWTPs. On the other hand, Plant C uses PACl-1.5s as a coagulant, whereas Plant D uses high-basicity PACl with basicity 2.1 (PACl-2.1s; see Section S1.3). Accordingly, we investigated the effect of coagulant type on virus reduction in lab-scale C–MF; the use of PACl-2.1s instead of PACl-1.5s increased the reduction ratios of PMMoV from 0.5–1.1-$\log_{10}$ to 1.6–3.5-$\log_{10}$ (Fig. S6b). This result indicates that coagulant type affected virus reduction efficiency in C–MF, and that the use of high-basicity PACl at Plant D was probably a reason for the higher reduction ratios of PMMoV at Plant D than at Plant C. We further investigated the usefulness of high-basicity PACls, particularly a non-sulfated one, for improving virus reduction efficiency in full-scale CS–RSF and C–MF. In lab-scale CS–RSF, the use of high-basicity PACls increased the reduction ratios of PMMoV from 2.9-$\log_{10}$ to 3.5–4.1-$\log_{10}$ (Fig.

448 S6a). In lab-scale C–MF, the PMMoV reduction ratios of >4-$\log_{10}$ were achieved by using non-
449 sulfated, high-basicity PACl at 0.27 mg-Al/L (Fig. S6b), similar to the dosage in C–MF at Plant C. In
450 addition, our research group has reported that coagulation pretreatment with high-basicity PACls
451 more effectively mitigates membrane fouling in MF than that with PACl-1.5s (Kimura et al., 2015).
452 Thus, the efficiency of virus reduction could be increased to >4-$\log_{10}$ in full-scale C–MF with a more
453 effective mitigation of membrane fouling by the use of non-sulfated, high-basicity PACl even at a
454 low dosage similar to those applied in full-scale C–MF (e.g., 0.27 mg-Al/L). Details of the effect of
455 coagulant type on virus reduction are described in Section S2.6.
456 Powdered activated carbon is injected into water after pre-chlorination at Plant D, but not Plant C.
457 Our research group has reported that the size of aluminum floc particles generated in C–MF clearly
458 increases in the presence of powdered activated carbon (Matsui et al., 2009). The addition of
459 powdered activated carbon likely generated larger floc particles during coagulation at Plant D than at
460 Plant C, although floc size was not measured in the present study. In general, large floc particles are
461 more effectively removed by the membrane than small floc particles. Thus, enhanced removal of floc
462 particles that entrapped viruses may explain the higher reduction ratios of PMMoV in C–MF at Plant
463 D than at Plant C. Further study is needed to investigate whether virus reduction ratios are actually
464 improved by the addition of powdered activated carbon in C–MF.
465
466 *3.5. Reduction of indigenous human enteric viruses in full-scale DWTPs employing CS–RSF and C–*
467 *MF*
468
469 We compared the reduction ratios of indigenous human enteric viruses (AdV, EVs including CV,
470 HAV, and HuNoVs GI and GII) with those of indigenous PMMoV in full-scale CS–RSF and C–MF.
471 Indigenous PMMoV was quantified in 100% (20/20) of the raw water samples, whereas indigenous
472 EVs were quantified in 25% (5/20; 0/7 for Plant A, 1/3 for Plant B, 4/5 for Plant C, 0/5 for Plant D)

473 and HuNoV GII in 15% (3/20; 0/7 for Plant A, 1/3 for Plant B, 0/5 for Plant C, 2/5 for Plant D) of the
474 samples (Fig. S7). Concentrations of indigenous AdV, HAV, and HuNoV GI in raw water were always
475 below the quantification limit.

476 At Plant B, the concentrations of indigenous EVs and HuNoV GII in treated water after CS and
477 after RSF were always below the quantification limit (Fig. 5a). The reduction ratios in CS–RSF were
478 ≥1.3-$\log_{10}$ for EVs and ≥1.5-$\log_{10}$ for HuNoV GII; both were higher than that of PMMoV (0.9-$\log_{10}$)
479 on the same day in February 2019. On this sampling day, pre-chlorination was applied before CS. CV
480 (included in EVs) is less resistant to chlorine treatment than PMMoV (Shirasaki et al., 2020), and
481 HuNoV is less resistant than PV (included in EVs; Shin and Sobsey, 2008). Thus, not only removal
482 of viral particles by CS–RSF but also degradation of viral genetic material by pre-chlorination could
483 reduce the PCR signal of EVs and HuNoV GII in CS–RSF at Plant B.

484 At Plant C, the concentrations of indigenous EVs in treated water after MnOx-coated media
485 filtration (i.e., water just before C–MF) were always below the quantification limit (Fig. 5b), so the
486 reduction ratios of EVs in C–MF could not be determined. At Plant D, the concentrations of
487 indigenous HuNoV GII in treated water after coagulation and after MF were always below the
488 quantification limit (Fig. 5c). We could not conclude whether the reduction ratios of HuNoV GII in
489 C–MF (≥1.5-$\log_{10}$) were higher than those of PMMoV (2.3–2.9-$\log_{10}$) on the same days in January
490 and March 2021.

491 In the present study, the concentrations of indigenous human enteric viruses in treated water after
492 CS–RSF or C–MF were always below the quantification limit, because of their low concentrations in
493 raw water and low resistance to chlorine treatment. Thus, it is difficult to directly evaluate their
494 reduction efficiencies in full-scale physical and physicochemical treatment processes (i.e., particle
495 separation processes), particularly when pre- and/or intermediate-chlorination is applied. In contrast,
496 indigenous PMMoV was always quantified even in treated water, owing to its high concentrations in
497 raw water and higher resistance to chlorine treatment than that of human enteric viruses including a

chlorine-resistant virus, CV (Shirasaki et al., 2020). In addition, our research group has reported that the reduction ratios of PMMoV are similar to or lower than those of AdV, CV, HAV, and the surrogate of human noroviruses, MNV, in lab-scale virus-spiking CS–RSF and LPM filtration experiments (Shirasaki et al., 2017a, 2018). Thus, PMMoV could be used as a potential surrogate for these viruses to assess their removal by full-scale physical and physicochemical treatment processes, even when pre- and/or intermediate-chlorination is applied. In full-scale CS–RSF and LPM filtration, reduction ratios of AdV, CV, HAV, and human noroviruses could be expected to be similar to or higher than those of PMMoV. This is supported by the higher reduction ratios of EVs and HuNoV GII in CS–RSF at Plant B than that of PMMoV.

4. Conclusions

(1) The developed virus concentration method by using an electropositive filter and TF-UF membrane effectively concentrated and recovered PMMoV from large volumes of water: total recovery rates of 33%–42% were maintained even when as much as 500–2000 L of PMMoV-spiked dechlorinated tap water was concentrated to 20 mL.

(2) The reduction ratios of indigenous PMMoV determined by using this method were 0.9–2.7-$\log_{10}$ in full-scale CS–RSF and 0.7–2.9-$\log_{10}$ in full-scale C–MF.

(3) The reduction ratios of PMMoV in C–MF at Plant C (1.0 ± 0.3-$\log_{10}$) were lower than those in CS–RSF at Plants A (1.7 ± 0.5-$\log_{10}$) and B (1.4 ± 0.7-$\log_{10}$), although MF has higher ability for particle separation than RSF. Lab-scale virus-spiking C–MF experiments that mimicked full-scale C–MF demonstrated that the low coagulant dosages applied in C–MF, which are determined mainly from the viewpoint of preventing membrane fouling, probably led to the lower reduction ratios in C–MF than in CS–RSF. This implies that higher virus reduction ratios

than those achieved in full-scale CS–RSF are not necessarily achieved in full-scale C–MF, despite its higher ability for virus reduction in comparison with CS–RSF.

(4) The reduction ratios of PMMoV in C–MF at Plant D (2.2 ± 0.6-$\log_{10}$) were higher than those at Plant C, despite similar coagulant dosages. In lab-scale C–MF, the PMMoV reduction ratios were improved from 1-$\log_{10}$ to 2–4-$\log_{10}$ by using high-basicity PACl instead of PACl-1.5s. Thus, the use of high-basicity PACl at Plant D probably resulted in higher reduction ratios of PMMoV in C–MF at Plant D than at Plant C.

(5) In contrast to human enteric viruses, indigenous PMMoV could always be quantified even in treated water, owing to its high concentrations in raw water and high resistance to chlorine treatment. Together with our previous findings of similar or lower reduction ratios of PMMoV in comparison with those of human enteric viruses in lab-scale virus-spiking CS–RSF and LPM filtration experiments, PMMoV could be used as a potential surrogate for human enteric viruses to assess virus removal by full-scale physical and physicochemical treatment processes, even when pre- and/or intermediate-chlorination is applied. This possibility is supported by higher reduction ratios of EVs (≥1.3-$\log_{10}$) and HuNoV GII (≥1.5-$\log_{10}$) than that of PMMoV (0.9-$\log_{10}$) in CS–RSF at Plant B, although it could not be judged whether the reduction ratios of HuNoV GII (≥1.5-$\log_{10}$) were higher than those of PMMoV (2.3–2.9-$\log_{10}$) in C–MF at Plant D.

Acknowledgements

This work was supported by the Japan Society for the Promotion of Science (grant numbers 19H02269, 2019; 16H06362, 2016; 18H03790, 2018); the Ministry of Health, Labor, and Welfare, Japan; the Bureau of Water Works, Tokyo Metropolitan Government, Japan; The River Foundation, Japan; and the FUSO Innovative Technology Fund, Japan.

547

548 **References**

549

550 Abbaszadegan, M., Mayer, B.K., Ryu, H., Nwachuku, N., 2007. Efficacy of Removal of CCL Viruses
551 under Enhanced Coagulation Conditions. Environ. Sci. Technol. 41, 971–977.
552 Asami, T., Katayama, H., Torrey, J.R., Visvanathan, C., Furumai, H., 2016. Evaluation of virus
553 removal efficiency of coagulation–sedimentation and rapid sand filtration processes in a drinking
554 water treatment plant in Bangkok, Thailand. Water Res. 101, 84–94.
555 Cashdollar, J.L., Brinkman, N.E., Griffin, S.M., McMinn, B.R., Rhodes, E.R., Varughese, E.A.,
556 Grimm, A.C., Parshionikar, S.U., Wymer, L., Fout, G.S., 2013. Development and evaluation of
557 EPA Method 1615 for detection enterovirus and norovirus in water. Appl. Environ. Microbiol. 79
558 (1), 215–223.
559 Fauquet, C.M., Mayo, M.A., Maniloff, J., Desselberger, U., Ball, L.A. (Eds.), 2005. Virus Taxonomy:
560 Eighth Report of the International Committee on Taxonomy of Viruses. Elsevier Academic Press,
561 London, UK.
562 Fout, G.S., Brinkman, N.E., Cashdollar, J.L., Griffin, S.M., McMinn, B.R., Rhodes, E.R., Varughese,
563 E.A., Karim, M.R., Grimm, A.C., Spencer, S.K., Borchardt, M.A., 2014. Method 1615:
564 Measurement of Enterovirus and Norovirus Occurrence in Water by Culture and RT-qPCR, Version
565 1.3. EPA/600/R-10/181. U.S. Environmental Protection Agency, Cincinnati, OH, USA.
566 Fiksdal, L., Leiknes, O., 2006. The effect of coagulation with MF/UF membrane filtration for the
567 removal of virus in drinking water. J. Membr. Sci. 279 (1–2), 364–371.
568 Hamza, I.A., Jurzik, L., Uberla, K., Wilhelm, M., 2011. Evaluation of pepper mild mottle virus,
569 human picobirnavirus and Torque teno virus as indicators of fecal contamination in river water.
570 Water Res. 45 (3), 1358–1368.

571 Haramoto, E., Kitajima, M., Hata, A., Torrey, J.R., Masago, Y., Sano, D., Katayama, H., 2018. A
572 review on recent progress in the detection methods and prevalence of human enteric viruses in
573 water. Water Res. 135, 168–186.
574 Haramoto, E., Kitajima, M., Kishida, N., Konno, Y., Katayama, H., Asami, M., Akiba, M., 2013.
575 Occurrence of pepper mild mottle virus in drinking water sources in Japan. Appl. Environ.
576 Microbiol. 79 (23), 7413–7418.
577 Health Canada, 2017. Guidelines for Canadian Drinking Water Quality: Guideline Technical
578 Document. Enteric Viruses in Drinking Water. Water and Air Quality Bureau, Health Canada,
579 Ottawa, Canada.
580 Huang, H., Schwab, K., Jacangero, J.G., 2009. Pretreatment for low pressure membranes in water
581 treatment: a review. Environ. Sci. Technol. 43 (9), 3011–3019.
582 Kato, R., Asami, T., Utagawa, E., Furumai, H., Katayama, H., 2018. Pepper mild mottle virus as a
583 process indicator at drinking water treatment plants employing coagulation–sedimentation, rapid
584 sand filtration, ozonation, and biological activated carbon treatments in Japan. Water Res. 132, 61–
585 70.
586 Katzenelson, E., Fattal, B., Hostovesky, T., 1976. Organic flocculation: an efficient second-step
587 concentration method for the detection of viruses in tap water. Appl. Environ. Microbiol. 32 (4),
588 638–639.
589 Kimura, M., Matsui, Y., Saito, S., Takahashi, T., Nakagawa, M., Shirasaki, N., Matsushita, T., 2015.
590 Hydraulically irreversible membrane fouling during coagulation-microfiltration and its control by
591 using high-basicity polyaluminum chloride. J. Membr. Sci. 477, 115–122.
592 Matsui, Y., Hasegawa, H., Ohno, K., Matsushita, T., Mima, S., Kawase, Y., Aizawa, T., 2009. Effects
593 of super-powdered activated carbon pretreatment on coagulation and trans-membrane pressure
594 buildup during microfiltration. Water Res. 43, 5160–5170.

595 Matsui, Y., Matsushita, T., Inoue, T., Yamamoto, M., Hayashi, Y., Yonekawa, H., Tsutsumi, Y., 2003.
596 Virus removal by ceramic membrane microfiltration with coagulation pretreatment. Water Sci.
597 Technol.: Water Supply. 3 (5), 93–99.
598 Matsushita, T., Shirasaki, N., Tatsuki, Y., Matsui, Y., 2013. Investigating norovirus removal by
599 microfiltration, ultrafiltration, and pre-coagulation–microfiltration processes using recombinant
600 norovirus virus-like particles and real-time immuno-PCR. Water Res. 47 (15), 5819–5827.
601 Sano, Y., Nozu, Y., Inoue, H., 1978. The interaction of sodium dodecyl sulfate with cucumber green
602 mottle mosaic virus protein and tobacco mosaic virus protein. Arch. Biochem. Biophys. 186 (2),
603 307–316.
604 Shi, H., Pasco, E.V., Tarabara, V.V., 2017. Membrane-based methods of virus concentration from
605 water: a review of process parameters and their effects on virus recovery. Environ. Sci.: Water Res.
606 Technol. 3, 778–792.
607 Shin, G.-A., Sobsey, M.D., 2008. Inactivation of norovirus by chlorine disinfection of water. Water
608 Res. 42, 4562–4568.
609 Shirasaki, N., Matsushita, T., Matsui, Y., Marubayashi, T., Murai, K., 2016. Investigation of enteric
610 adenovirus and poliovirus removal by coagulation processes and suitability of bacteriophages MS2
611 and φX174 as surrogates for those viruses. Sci. Total Environ. 563, 29–39.
612 Shirasaki, N., Matsushita, T., Matsui, Y., Murai, K., 2017a. Assessment of the efficacy of membrane
613 filtration processes to remove human enteric viruses and the suitability of bacteriophages and a
614 plant virus as surrogates for those viruses. Water Res. 115, 29–39.
615 Shirasaki, N., Matsushita, T., Matsui, Y., Murai, K., Aochi, A., 2017b. Elimination of representative
616 contaminant candidate list viruses, coxsackievirus, echovirus, hepatitis A virus, and norovirus,
617 from water by coagulation processes. J. Hazard. Mater. 326, 110–119.

618 Shirasaki, N., Matsushita, T., Matsui, Y., Yamashita, R., 2018. Evaluation of the suitability of a plant
619 virus, pepper mild mottle virus, as a surrogate of human enteric viruses for assessment of the
620 efficacy of coagulation–rapid sand filtration to remove those viruses. Water Res. 129, 460–469.
621 Shirasaki, N., Matsushita, T., Matsui, Y., Koriki, S., 2020. Suitability of pepper mild mottle virus as
622 a human enteric virus surrogate for assessing the efficacy of thermal or free-chlorine disinfection
623 processes by using infectivity assays and enhanced viability PCR. Water Res. 186, 116409.
624 Sylvestre, E., Prevost, M., Burnet, J.B., Pang, X., Qiu, Y., Smeets, P., Medema, G., Hachad, M.,
625 Dorner, S., 2021. Demonstrating the reduction of enteric viruses by drinking water treatment during
626 snowmelt episodes in urban areas. Water Res. X. 11, 100091.
627 USEPA (U.S. Environmental Protection Agency), 2016. Drinking Water Contaminant Candidate List
628 4. EPA-HQ-OW-2012-0217. Office of Water, U.S. Environmental Protection Agency, Washington,
629 DC, USA.
630 Varughese, E.A., Brinkman, N.E., Anneken, E.M., Cashdollar, J.L., Fout, G.S., Furlong, E.T., Kolpinc,
631 D.W., Glassmeyer, S.T., Keely, S.P., 2018. Estimating virus occurrence using Bayesian modeling
632 in multiple drinking water systems of the United States. Sci. Total Environ. 619–620, 1330–1339.
633 WHO (World Health Organization), 2011. Guidelines For Drinking-Water Quality, 4th ed. World
634 Health Organization, Genava, Switzerland.
635 Zhu, B., Clifford, D.A., Chellam, S., 2005. Virus removal by iron coagulation–microfiltration. Water
636 Res. 39 (20), 5153–5161.
637
638

Table 1

Effects of filter type, pH of beef extract solution, and soaking times before the third and fourth elution on retention rate of PMMoV on NanoCeram filters, its elution rate from the filters with beef extract solution, and total recovery rate of PMMoV from 1000 L of PMMoV-spiked dechlorinated tap water. The experimental conditions of Method 1615 are as follows: filter type, VS2.5-5; pH of beef extract solution, 9.0; number of virus elution procedures, two; soaking times before the first and second elution, 1 and 15 min, respectively; tangential-flow ultrafiltration, not included.

Method	Filter type	pH of beef extract solution	Soaking time (min)				Tangential-flow ultrafiltration	Retention rate R_r (%)	Elution rate R_e (%)	Total recovery rate R_t (%)
			First	Second	Third	Fourth				
1	P2.5-5DP	9.0	1	15	15	15	−	94.8	27.5	0.7
2	P2.5-5DP	9.0	1	15	30	30	+[a]	99.6	32.1	48.8
3	P2.5-5DP	9.5	1	15	30	30	+	98.8	59.6	78.4
4	VS2.5-5	9.5	1	15	30	30	+	96.8	74.1	80.3

[a] + indicates that tangential-flow ultrafiltration was added to the virus concentration processes.

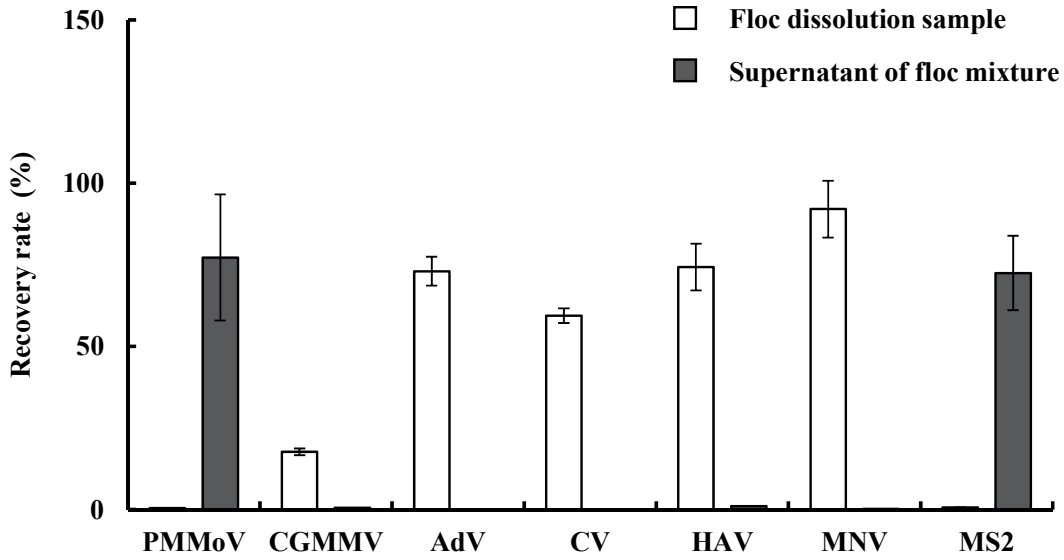

Fig. 1 – Behavior of the viruses during organic flocculation. Viruses were spiked to the BE solution (pH 9.5) at initial concentrations of $10^{8–9}$ copies/mL for PMMoV, $10^{7–8}$ copies/mL for CGMMV, CV, and MNV, 10^{7} copies/mL for AdV, 10^{6} copies/mL for HAV, and 10^{10} copies/mL for MS2. Values are means and error bars indicate standard deviations (n = 3).

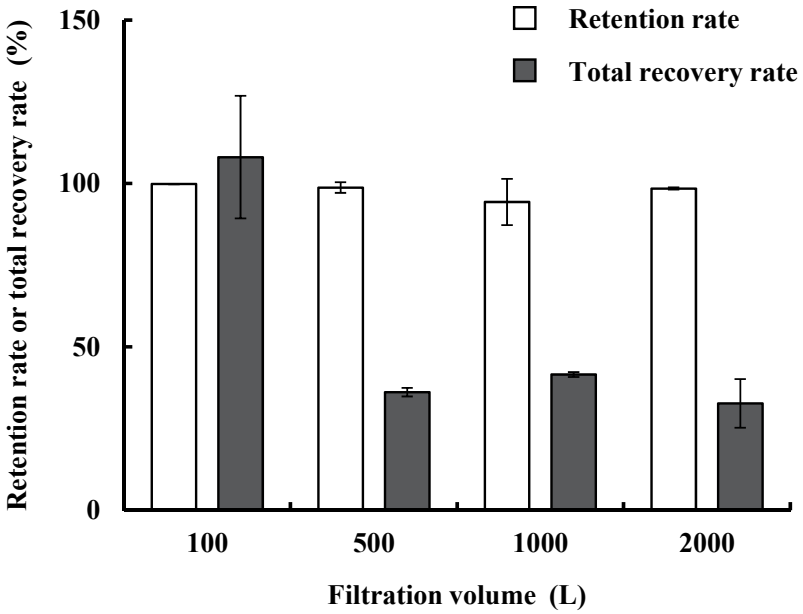

656

657

658 **Fig. 2 – Effect of filtration volume on retention rate of PMMoV on NanoCeram filters and total**

659 **recovery rate of PMMoV from PMMoV-spiked dechlorinated tap water.** Initial concentration of

660 PMMoV, 10^8 copies/mL. Values are means and error bars indicate standard deviations (n = 2 or 3).

661

662

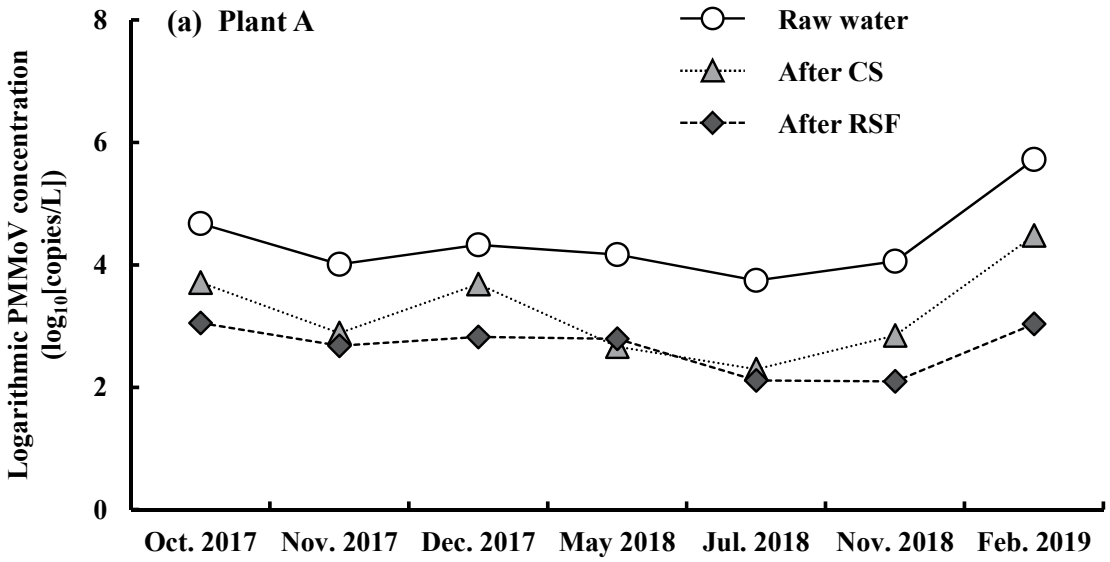
(a) Plant A
Logarithmic PMMoV concentration
(log_{10}[copies/L])
8
6
4
2
0
Oct. 2017
Nov. 2017
Dec. 2017
May 2018
Jul. 2018
Nov. 2018
Feb. 2019
Raw water
After CS
After RSF

663

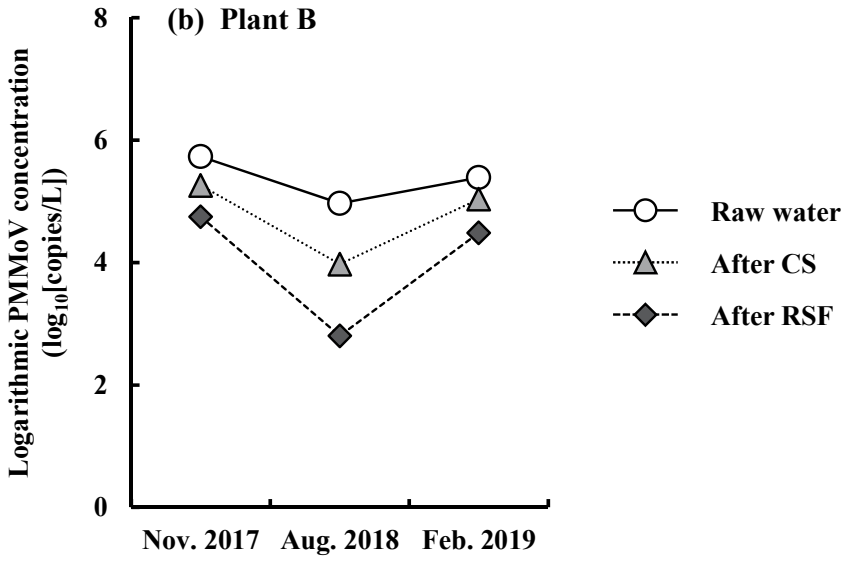
(b) Plant B
Logarithmic PMMoV concentration
(log_{10}[copies/L])
8
6
4
2
0
Nov. 2017
Aug. 2018
Feb. 2019
Raw water
After CS
After RSF

664

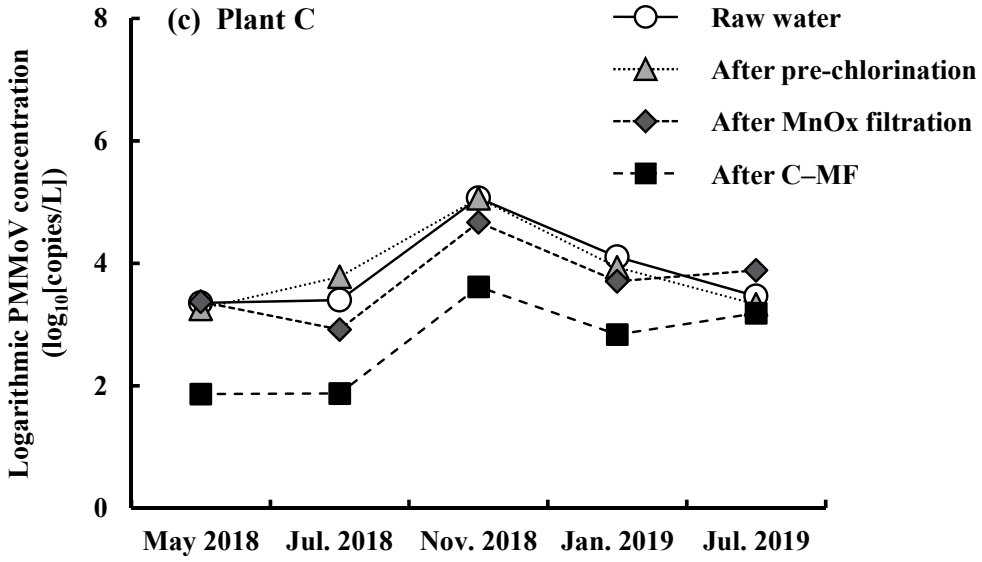
(c) Plant C
Logarithmic PMMoV concentration
(log_{10}[copies/L])
8
6
4
2
0
May 2018
Jul. 2018
Nov. 2018
Jan. 2019
Jul. 2019
Raw water
After pre-chlorination
After MnOx filtration
After C–MF

665

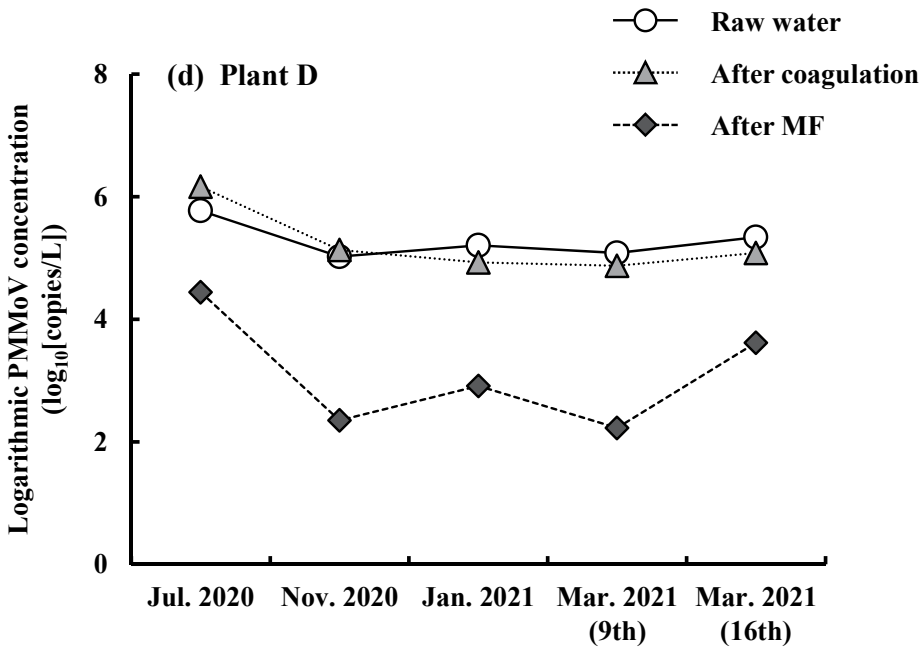

666

667

668 **Fig. 3 – Concentrations of indigenous PMMoV in raw and treated water at Plants A (a), B (b),**

669 **C (c), and D (d).** Samples of raw water and treated water after coagulation (4 or 20 L) collected at

670 Plant D in July 2020 were concentrated in our laboratory, not on-site.

671

672

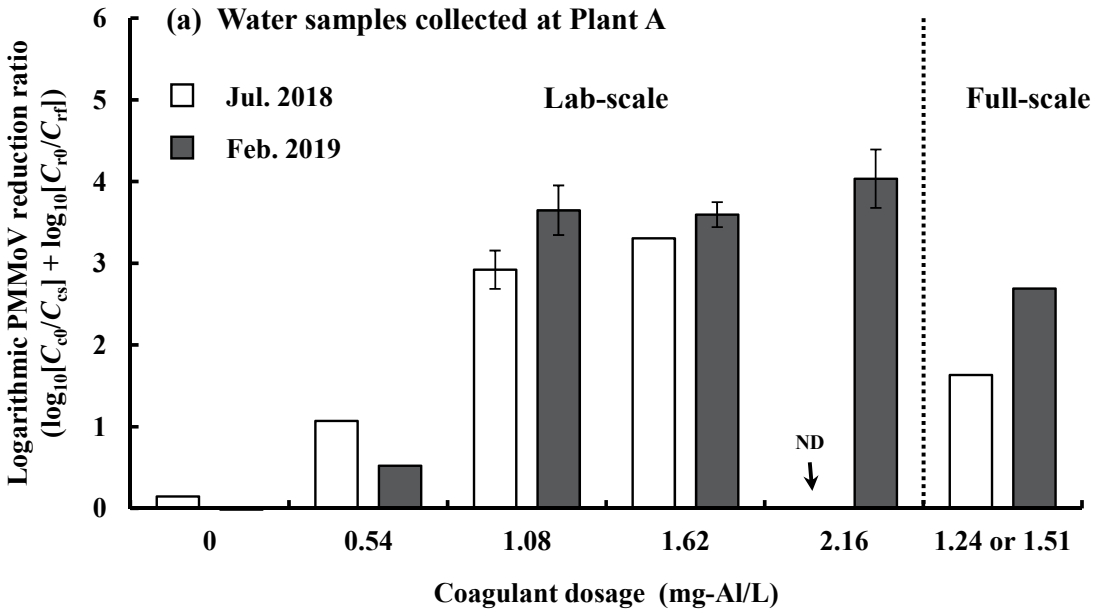
(a) Water samples collected at Plant A
Jul. 2018
Feb. 2019
Lab-scale
Full-scale
ND
Logarithmic PMMoV reduction ratio
(log10[Cc0/Ccs] + log10[Cr0/Crf])
0
1
2
3
4
5
6
0
0.54
1.08
1.62
2.16
1.24 or 1.51
Coagulant dosage (mg-Al/L)

673

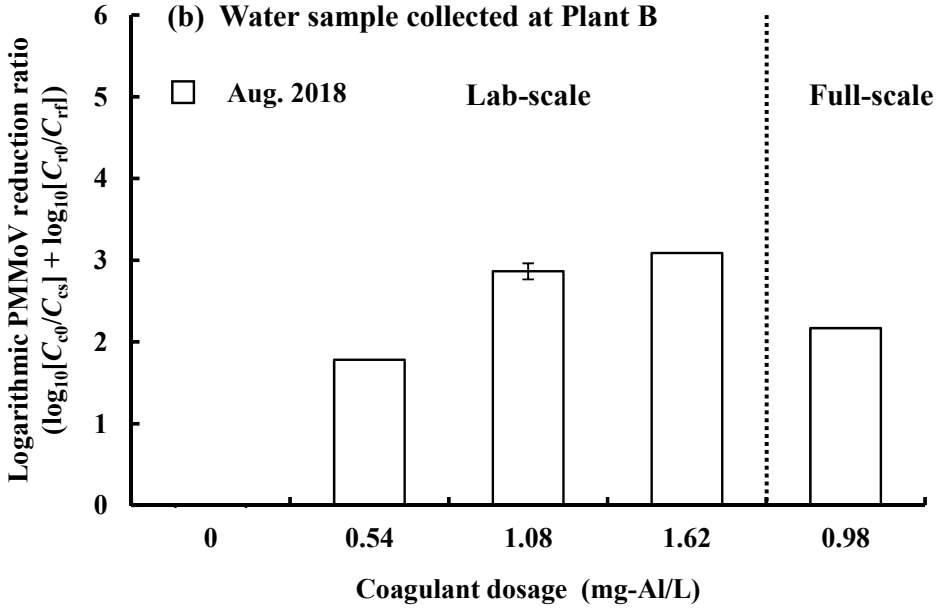
(b) Water sample collected at Plant B
Aug. 2018
Lab-scale
Full-scale
Logarithmic PMMoV reduction ratio
(log10[Cc0/Ccs] + log10[Cr0/Crf])
0
1
2
3
4
5
6
0
0.54
1.08
1.62
0.98
Coagulant dosage (mg-Al/L)

674

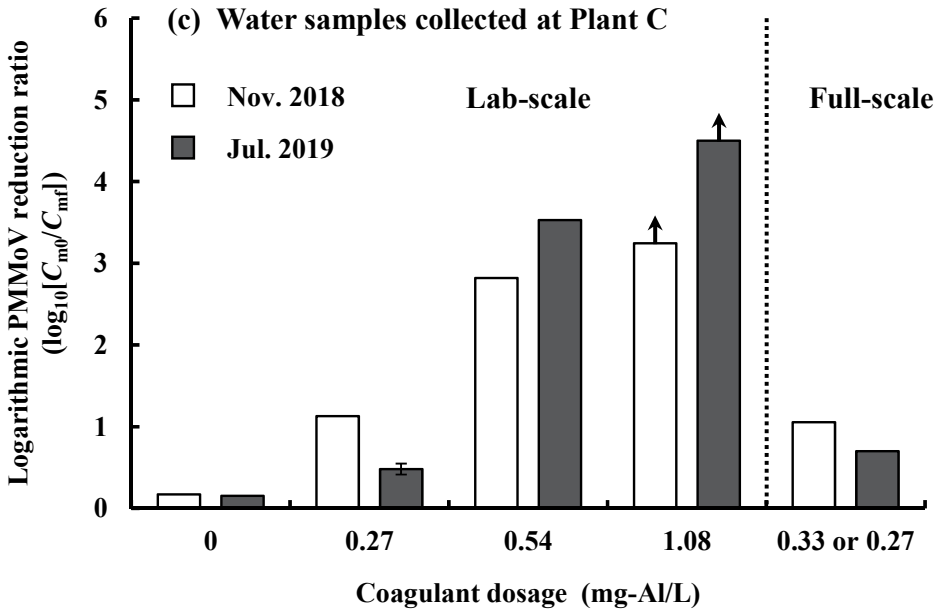

675

676

677 **Fig. 4 – Effect of coagulant dosage on reduction ratios of PMMoV in lab-scale CS–RSF (a, b)**
678 **and C–MF (c).** Raw water samples collected at Plant A in July 2018 and February 2019 (a), and Plant
679 B in August 2018 (b), and treated water samples after MnOx-coated media filtration collected at Plant
680 C in November 2018 and July 2019 (c) were spiked with PMMoV at an initial concentration of $10^{7–}$
681 ^{8} copies/mL, and then used as experimental raw water. Coagulant, PACl-1.5s. Manganese sand (a) or
682 silica sand (b) was used. Values are means and error bars indicate standard deviations (n = 1–3).
683 Arrows indicate that the virus concentrations were below the limit of quantification of the real-time
684 RT-PCR. ND, not determined.

685

686

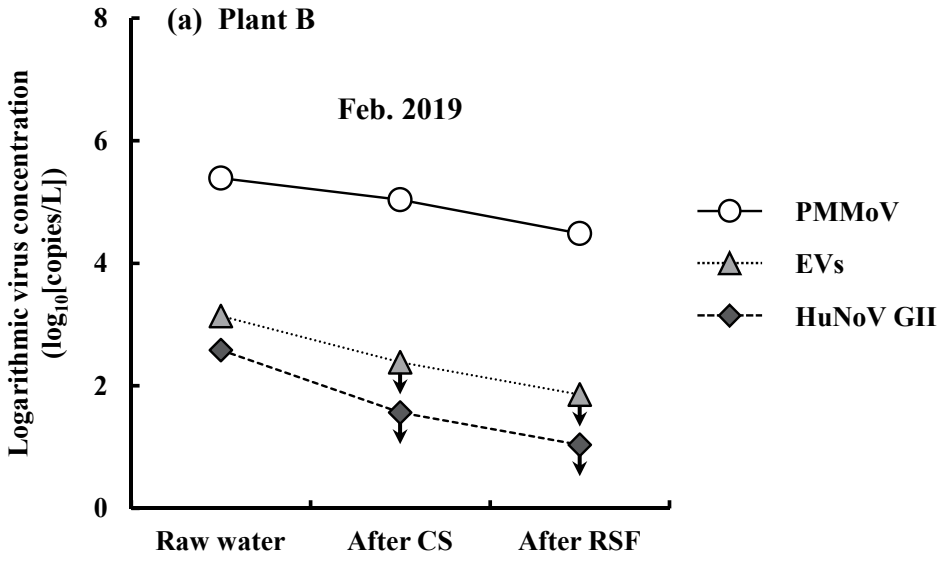
(a) Plant B
Feb. 2019
Logarithmic virus concentration
(log10[copies/L])
8
6
4
2
0
Raw water
After CS
After RSF
PMMoV
EVs
HuNoV GII

687

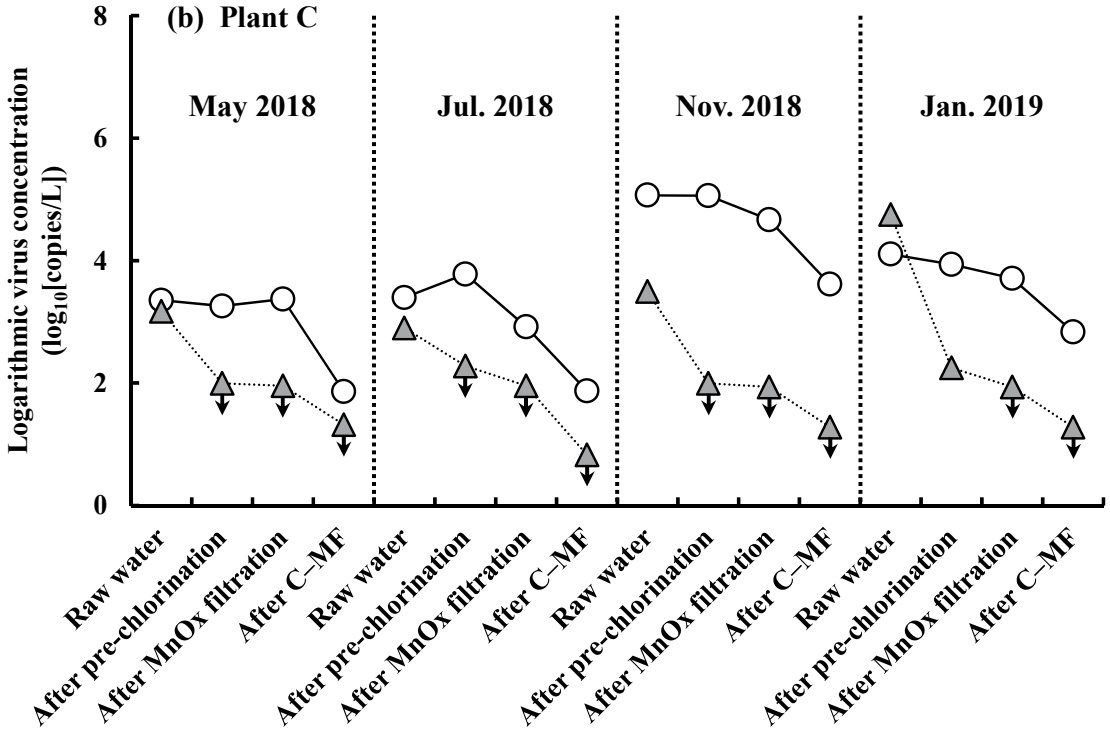
(b) Plant C
May 2018
Jul. 2018
Nov. 2018
Jan. 2019
Logarithmic virus concentration
(log10[copies/L])
8
6
4
2
0
Raw water
After pre-chlorination
After MnOx filtration
After C–MF

688

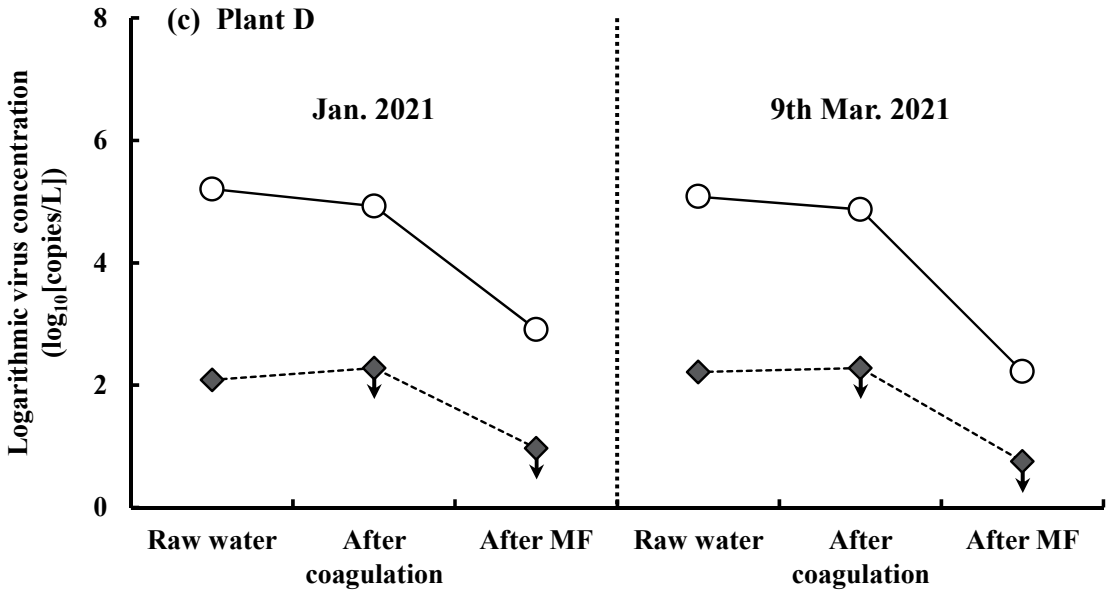

689

690

691 **Fig. 5 – Concentrations of indigenous PMMoV and human enteric viruses in raw and treated**
692 **water at Plants B (a), C (b), and D (c).** Treated water samples were tested only when at least one
693 indigenous human enteric virus could be quantified in raw water samples. Arrows indicate that the
694 virus concentrations were below the limit of quantification of the real-time RT-PCR.

695